Review paper

HIGH TEMPERATURE MECHANICAL PROPERTIES OF Al-Al$_4$C$_3$ COMPOSITE PRODUCED BY MECHANICAL ALLOYING

Michal Besterci[1), Ferdinand Dobeš[2), Tibor Kvačkaj[3), Katarína Sülleiová[1), Beata Ballóková[1) , Oksana Velgosová[4)

[1)*Institute of Materials Research, Slovak Academy of Sciences, Watsonova 47, 040 01 Košice, Slovakia*

[2)*Institute of Physics of Materials, Academy of Sciences of the Czech Republic, Žižkova 22, 616 62 Brno, Czech Republic*

[3)*Department of Metal Forming, Faculty of Metallurgy, Technical University of Košice, Vysokoškolská 4, 042 00 Košice, Slovakia*

[4)*Department of Material Science, Faculty of Metallurgy, Technical University of Košice, Letná 9, 042 00 Košice, Slovakia*

Corresponding author: Michal Besterci, e-mail: mbesterci@imr.saske.sk, Tel.: +421 55 792 2441 , Institute of Materials Research, Slovak Academy of Sciences, Watsonova 47, 040 01 Košice, Slovakia

Abstract

A method of mechanical alloying process is described. It was proved that the transformation efficiency of carbon to Al$_4$C$_3$ by heat treatment of aluminium with the porous furnace black and electrographite at temperatures 723 – 873 K and time periods 1 - 10 hours is higher than that of the hard cracked graphite. The size of Al$_4$C$_3$ dispersed phase was measured on thin foil and it was constant and as small as 30 nm. Subgrain size measured in the range of 100 grains in thin foils depended on the carbon type.. It ranged from 0.3 to 0.7 μm. Mechanical properties were analyzed in a microstructural matrix (after extrusion) as well as in nano-matrix The temperature dependence of ductility, and reduction of area in the temperature range of 623 – 723 K and strain rate of 10^{-1} s^{-1}, indicated a considerable increase of properties. In a case when the volume fraction of Al$_4$C$_3$ changes from lower to higher, the grain rotation mechanism dominates instead of the grain boundary sliding. Creep parameters for Al-Al$_4$C$_3$ systems and commercial IN9021 and IN9052 systems were compared. The dependence of the minimum deflection rate on the applied force as well as the dependence of the time to fracture on the applied force for two temperature levels (623 and 723 K) by small punch testing is depicted. The anisotropy of the creep properties and fracture using small punch tests for the Al-Al$_4$C$_3$ system produced by ECAP were analyzed.

1 Introduction

Since strengthening of aluminium alloys by (noncoherent) Al$_4$C$_3$ particles can be expected to have great potentiality for increasing their high temperature mechanical properties, creep and creep fracture in such alloys have been investigated extensively [1, 2]. Aluminium alloys strengthened by Al$_4$C$_3$ particles are produced by mechanical alloying and/or reaction milling

followed by consolidation and hot extrusion. The alloys are typically fine grained (the mean grain diameter is always less than 1 μm) and always contain a volume fraction of Al_2O_3 particles besides that of Al_4C_3, [3]. The particles size is typically 20 nm.

Mechanical alloying is the process of production of macroscopically homogeneous materials from heterogeneous mixtures. The process is implemented in laboratories in attritors, on the industrial scale in high energy ball mills. It is based on deformation, repeated disintegration and welding of power particles during intensive dry milling [4, 5]. Originally, this technology was developed for production of Ni and Fe superalloys. Later, it was shown that mechanical alloying is capable of producing several stable and metastable phases, including solid solutions, metastable crystalline and quasicrystalline phases, as well as amorphous phases. It is remarkable that the crystalline phases are usually of the nanometric size. Because these effects are similar to other ones, obtained by nonequilibrium techniques, such as rapid melt solidification, the system is characterized by increased mechanical properties. The advantage of preparing amorphous materials by mechanical alloying in comparison with rapid solidification technology is the fact that it allows larger quantities of materials to be produced, and the possibilities for alloying have therefore been extended. Mechanical alloying technology is now applied to different types of material systems, namely metals, ceramic and polymers, and considerable attention is being paid to it throughout the world. In the literature, the term for mechanical alloying is stated as ´mechanical alloying´ if elementary powders are used, and as ´mechanical milling´ if a pre-alloyed powder is used as the starting material. A series of material systems has been developed using mechanical alloying, mainly for high-temperature applications [6].

The aim of this paper is to study the influence of the various graphite types (when mixed with Al powder) and heat treatment procedure on the microstructure, mechanical properties and fracture of dispersion strengthened aluminium alloys in the Al_4C_3 system with micro and nanostructures.

2   Experimental material and methods

The experimental material - dispersion strengthened aluminium with Al_4C_3 particles was prepared by intense milling of aluminium powder with different types of carbon, as shown in **Table 1**. The prime aluminium powder grain size was 100 μm with the carbon content of 0.6 - 3 wt. %.

Table 1 Types of different carbon types

Notation	Type	Commercial Carbon
A	a_1	LTD
B	a_1	Spezialschwarz 5
C	a_1	Spezialschwarz 500
D	a_1	Printex 30
E	a_2	Printex 400
F	a_2	Farbruss FW 2
G	a_2	Flammruss 101
H	c	Thermax
I	b	Grafit KS 2.5

The aluminium composite dispersion strengthened by Al_4C_3 particles has been prepared by the method of mechanical alloying. The milling time used in all tested specimens was 90 min. The final carbide content was in the range of 2.5 – 12 vol. %. The obtained mixture was compacted

at 600 MPa and heat treated at 723, 773, 823, and 873 K whereas treatment times of 1, 3, 10, and 30 hours were employed. The final compacting by hot extrusion at a temperature of 823 K and a reduction of 94 % in the cross circular section of extruded bars was applied [7]. The experimental material has been prepared at the Institute for Chemical Technology of Inorganic Materials, TU Vienna.

A microstructural material Al-Al_4C_3 with 4 vol. % of Al_4C_3 was transformed by the ECAP (equal channel angular pressing) method by two passes into a nanocomposite material. The experimental material was pressed through two right angled (90°) channels of a special die by route "C", [8, 9]. The ECAP technology allows obtaining the very fine-grained micorstructure – nanostructure by multiple pressing through the die, **Fig. 1**.
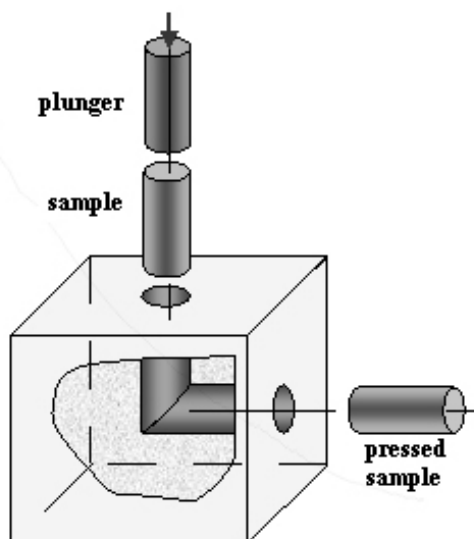
   Fig. 1   Scheme of ECAP

3   Results and discussion
3.1 Milling and carbonisation kinetics

The dependence of the transformation rate on temperature and holding time for the four carbon types is shown in **Fig. 2**. The good susceptibility to transformation for porous furnace black (a_1 and a_2) and that of electro-graphite (b) is evident. The porous carbon types are incorporated into the matrix by friction during milling, the distribution is uniform, and clustering is small. On the other side, hard graphite (c) resists disintegration and the granules are large.

Light microscopy microstructure analysis of the produced compacts proved a high homogeneity of dispersed particle distribution in the direction perpendicular to the direction of hot extrusion. In the longitudinal direction of the bar as a result of hot extrusion the Al_4C_3 carbide particles were arranged into bands.

During the milling of Al-1C system with the carbon type I microstructure changes occurred in the fracture processes and welding of the particles with incorporation of C phase and forming of final granules.
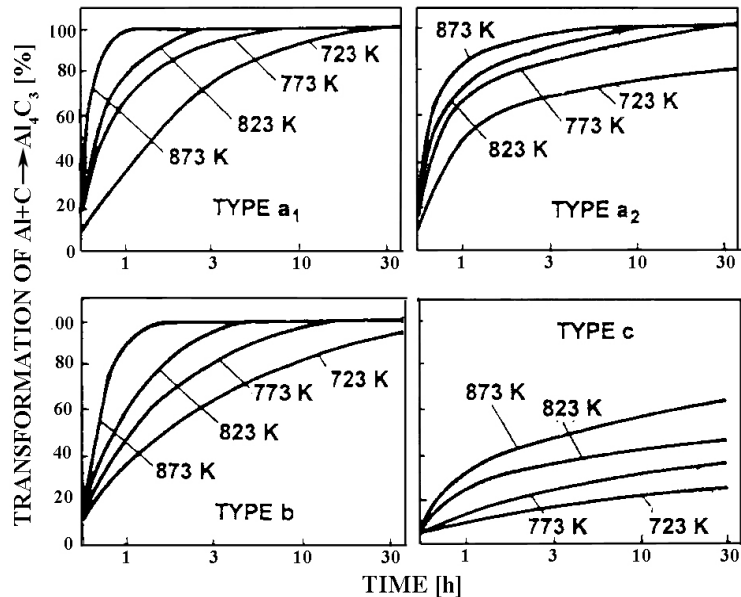
Fig. 2   Dependence of carbon to the carbide transformation rate on heat treatment temperature and holding time for four carbon types

The following micromechanisms, which take place during mechanical alloying, have been defined as the decisive ones:

1. Plastic deformation and deformation strengthening of the starting Al powders and their transformation to Al lamellae.
2. Creation of non-equiaxial aggregates from powder particles of the lamellae by the mechanism of cold welding with the origin of coherence failures being the same.
3. Forming and compacting of non-equiaxial aggregates and their transformation to equiaxial ones.
4. Exhaustion of deformability of aggregates or granules and their crumbling activated by weak surfaces on their structure.

Electron microscopy analysis was conducted using carbon replicas and thin foils. TEM of thin foils offered better results. For all the tested carbon combinations from the A to I labels, thin foils were produced for the heat treatment 723 K/30 h. The Al_4C_3 particle size and the subgrain size were measured using the thin foils. The dispersed phase Al_4C_3 particle size was measured on 100 to 200 thin foil structures, and it was constant and as small as 30 nm. The particle size was influenced neither by the carbon type nor by the heat treatment applied. Subgrain size measured in the range of 100 grains in thin foils depended on the carbon type, as well. It ranged from 0.3 to 0.7 μm. The stability of properties, resulting from graphite type I (KS 2.5), led to the highest production and utilization of this type of dispersion strengthening, [10].

3.2   Mechanical properties of microstructural system

In our previous works [11-13], we have evaluated the distance between the particles by point object simulation methods. This includes the mean interparticle distance λ_μ, the mean minimum

distance λ_ρ, the mean visibility λ_v, and the mean free spherical contact distance λ_ϑ. The characteristics and properties of these parameters have been analyzed in [11]. The mean free spherical contact distance λ_ϑ is the optimal parameter which has a physical interpretation, too.

During the last years, a new approach to the description of point systems has been developed intensively, which is referred to as polygonal methods [13]. The dual representation formed in the above way describes completely the given point system. Properties of Voronoi tessellation and their various generalizations are being very intensively studied now the state of this study is given in the monograph [14]. Intermediate stages of evaluation for thin foil (a), outlines of particles (b), and of reference points (c) are documented in **Fig. 3**.

The Al-Al$_4$C$_3$ system with 4 vol. % of Al$_4$C$_3$ was tested under different tensile conditions, where three different strain rates and different testing temperatures up to 723 K were used [15-16].
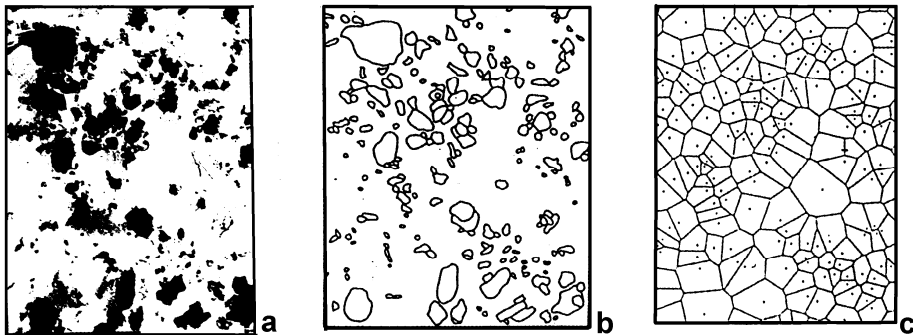
Fig. 3   Intermediate stages of evaluation for thin foil (a), outlines of particles (b), and reference points (c)

The results are shown in **Fig. 4**. The deformation mechanism and fracture mechanism were analyzed corresponding to different testing conditions. For the higher strain rates of 10^{-1}s^{-1} at 723 K, a significant growth of plastic properties was observed. The high uniform elongation A_5 of the specimen gauge length, and corresponding reduction values of the reduction in area Z were manifested in **Fig. 5**.
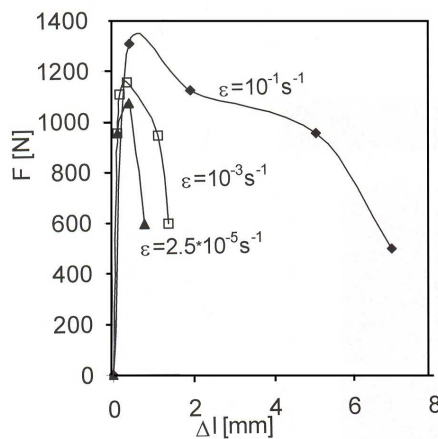
Fig. 4   Stress-strain dependences at 723 K ($\blacklozenge$ $\dot{\varepsilon}$ =10^{-1} s^{-1}, $\square$ $\dot{\varepsilon}$ =10^{-3} s^{-1}, $\blacktriangle$ $\dot{\varepsilon}$ =2.5$\cdot$10^{-5} s^{-1})
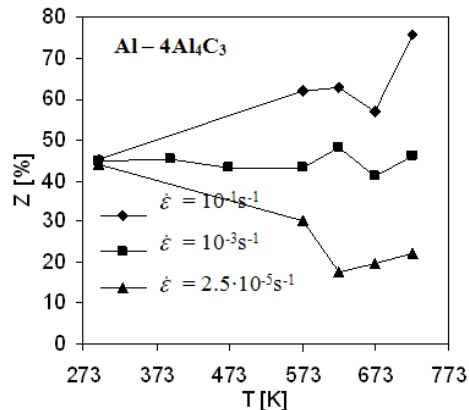
Fig. 5   Reduction of area Z as a function of strain rate and temperature

The ductility anomalies are showing an onset of a type of superplasticity. According to [17-19] it was proved that for materials Al - $12Al_4C_3$, the main mechanism responsible for superplastic behaviour is the grains rotation process and not sliding.

The comparison of real F-Δl curves for material Al-Al_4C_3 with 12% Al_4C_3 is given in **Fig. 6**. In the curves for 293 and 573 K the first part with deformation strengthening is followed immediately by the loss of plastic stability, plastic deformation localization and fracture. On the other side curves for high strain rate and temperatures of 673 and 723 K showed after part *I*, a definitely linear part *II* with near constant true stress, sometimes called „plateau", with dynamic recovery, and only after that the part *III*, with the loss of plastic stability.

The plastic properties for different strain rates are expressed by ductility A_5 in **Fig. 7**. For low strain rates a decrease of plastic properties is characteristic with the increase of temperature up to 723 K. A peak like significant increase of plastic properties is visible at 673 and 723 K in all plots (Fig. 8) for the highest strain rate $\dot{\varepsilon} = 1 \cdot 10^{-1} \, s^{-1}$. According to our experience, ductility A_5 is influenced by differences of deformation, and fracture in part *III* of the test. Cut-outs and thin foil TEM micrographs were produced also from the fracture area. The total values of ductility and reduction of area are much lower than those for known superplastic materials.
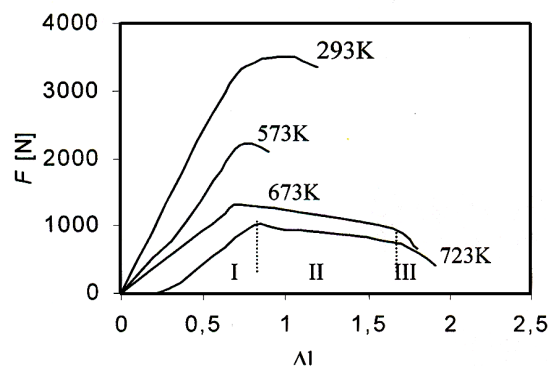
Fig. 6   Comparison of real F-Δl curves of the composite materials Al-Al_4C_3 for temperatures from 293 to 723 K and strain rate of $10^{-1}s^{-1}$
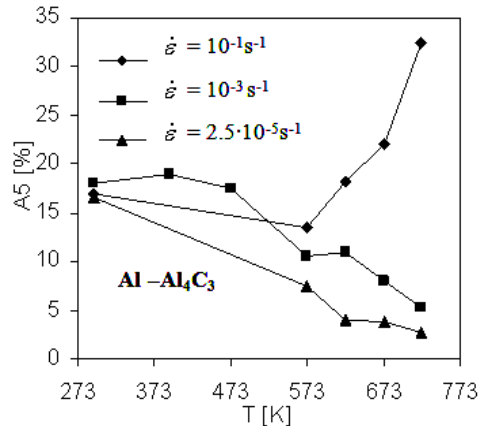
Fig. 7   Dependence of ductility on temperature and strain rate for Al-Al$_4$C$_3$ material at temperatures from 293 to 723 K and different strain rates

According to our previous results as well as those described in references, it appears that the deformation in the present Al-Al$_4$C$_3$ system includes and combines the following mechanisms:

a)   dynamic polygonization by dislocation migration and annihilations,
b)   slip on grain boundaries,
c)   displacement of grains by rotation,
d)   partial recrystallization causing grain boundary movement of polygonized grains,
e)   dislocation creep, causing accommodations of defects on grain boundaries (first in ternary points).

The partial contributions of different mechanisms to the total superplastic deformation. were analyzed. It was supposed that at high strain rate ($1.10^{-1} s^{-1}$) and high dispersed phase content (12 vol. % of Al$_4$C$_3$) dynamic recovery is started by the high accumulated deformation energy, then dynamic polygonization of grains, repositioning by rotation (no elongated grains seen), partial recrystallization and dislocation creep can take place, too. Clusters of particles identified as Al$_4$C$_3$ in **Fig. 8** on grain boundaries suggested more rotation than slip. For low dispersed phase particle content (4 vol. % of Al$_4$C$_3$) the elongated grains and slip on grain boundaries are more frequent, with lower probability of polygonization and partial recrystallization, **Fig. 9**. Grains can move or be reordered as shown in **Fig. 10** by the two mechanisms: a) slip along the grain boundaries, b) rotation.

During deformation of samples with high dispersed phase content at high strain rate, the recovery is not as perfect as known for superplastic materials. Local deformation with neck formation and fracture with limited reduction of area are the signs showing the limits of these materials. We suggest characterizing more precisely the deformation process in the Al-Al$_4$C$_3$ system in terms of quasi-superplastic behaviour.

The comparison of the test results and changes in fracture for the Al-Al$_4$C$_3$ system   at temperatures from 293 to 673 K and strain rates from $\dot{\varepsilon} = 2.5 \cdot 10^{-5}$ s^{-1} to $\dot{\varepsilon} = 1 \cdot 10^{-1}$ s^{-1} is summarized in [20].

The composition of the alloys investigated is given in **Table 2**. The alloys IN9021 and IN9052 were commercially produced by NOVAMET Co., USA, and supplied in the form of extruded bars 45 mm in diameter. The Al-Al$_4$C$_3$ alloys were laboratory produced at the Technical University Vienna, and supplied as extruded bars of 6 mm in diameter, [21].
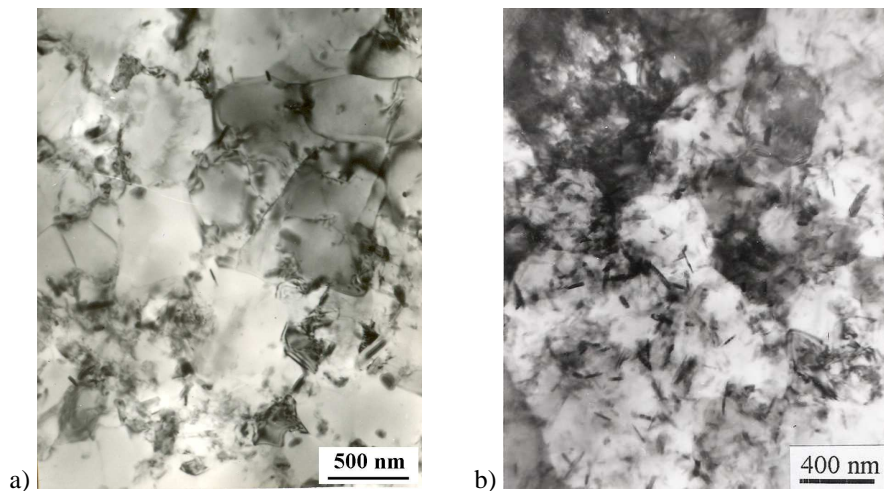
Fig. 8   Submicrostructure (foil) of Al-12Al$_4$C$_3$ material, (a) the transverse direction, (b) longitudinal direction
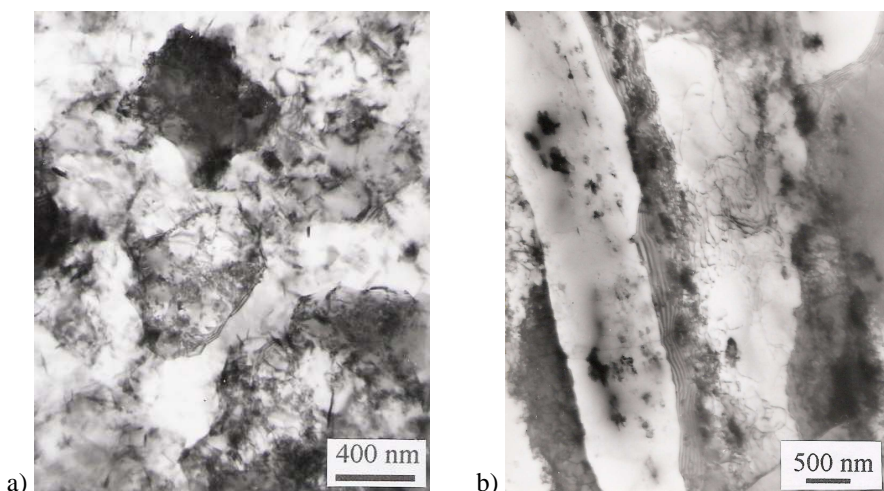
Fig. 9   TEM micrograph of the substructure of Al-4Al$_4$C$_3$ in the transverse direction (a), and in the longitudinal direction (b)

a)   **b)**
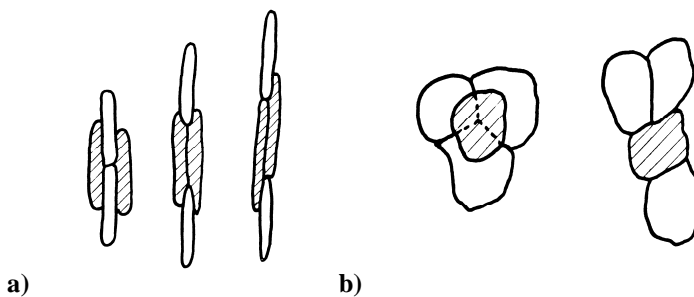
Fig. 10   Supposed reordering mechanisms: a) slip, b) rotation

Table 2 Dispersion strengthened aluminium alloys investigated: Nominal composition, grain size d, apparent activation energies of creep Q_c and creep fracture Q_f, apparent stress exponent of steady state creep rate m_c and of time to creep fracture m_f

Alloy [+])	d[μm]	Q_c[kJ.mol^{-1}]	Q_f[kJ.mol^{-1}]	m_c	m_f
IN9021 4.0Cu-1.5Mg- 4.5Al$_4$C$_3$ + 1.8Al$_2$0$_3$	0.86[++])	712 ± 40	574 ± 36	16.2 ± 36	15.2 ± 1.2
IN9021 4.0Cu- 0.5Si- 4.5 Al$_4$C$_3$ +1.8 Al$_2$0$_3$	0.55[+++]	398 ± 11	269 ± 13	12.2 ± 0.4	10.9 ± 0.4
Al-A l$_4$C$_3$ 2.5Al$_4$C$_3$ + 2.1Al$_2$0$_3$	0.82[+++]	268 ± 19	247 ± 19	21.5 ± 0.9	18.4 ± 1.0
Al-A l$_4$C$_3$ 10.0Al$_4$C$_3$ + 3.8Al$_2$0$_3$	0.72[+++]	275 ± 19	264 ± 18	20.7 ± 0.8	18.1 ± 0.8

[+])   Cu, Mg and Si in wt. %, Al$_4$C$_3$ and Al$_2$0$_3$ in vol. %
[++])   after annealing at 773 K for 14,4 ks
[+++])   in as received condition

In **Fig. 11**, relations between the "mean creep rate" ε_c / t_f and steady state creep rate $\dot{\varepsilon}_s$ is shown for the Al-Al$_4$C$_3$ alloys at temperatures 623 K and 723 K; ε_c is the creep strain to fracture. It can be seen that the well known Monkman-Grant relation as modified introducing ε_c [22] holds:

$$\frac{\varepsilon_c}{f} = C \cdot \dot{\varepsilon}_s^p \quad , \tag{1.}$$

where C and p are constants; $p = 0.99 \pm 0.10$ for both alloys, too [23]. The fact that $Q_f < Q_c$ and $m_f < m_c$ is related to the temperature and stress dependence of the strain to fracture ε_c.
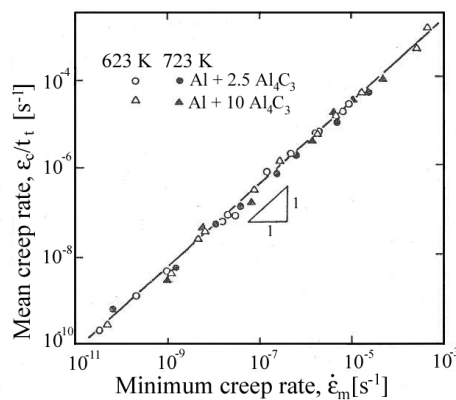
Fig. 11   Relation between "mean" creep rate and steady state creep rate for Al-Al$_4$C$_3$ alloys at temperatures 623 K and 723 K

At low stresses, to which long times to fracture correspond, the creep fracture is intergranular. As shown elsewhere [24], the validity of eqn. (1) with $p \sim 1$ strongly suggests the constrained intergranular cavity growth as one of the basic processes in creep fracture.

Creep behaviour of the composite based on aluminium matrix, reinforced by 4 vol. % Al_4C_3 was studied at temperatures from 623 to 723 K by small punch (SP) testing with a constant force. SP technique represents one of the recent methods for estimation of mechanical properties of solids [25, 26]. The time dependence of the central deflection was registered and the minimum deflection rate was determined.

The dependence of this quantity on the applied force can be described by a power function with relatively high value of the power. The dependence can be rationalized by an analysis in terms of the threshold concept. Analytical procedure for comparison of the threshold force in small punch experiments and threshold stress in conventional creep testing are given.

The dependence of the minimum deflection rate on the applied force for two temperature levels is given in **Fig. 12** in bilogarithmic coordinates. The dependence of the time to fracture, t_F on the applied force F is given in **Fig.13**.
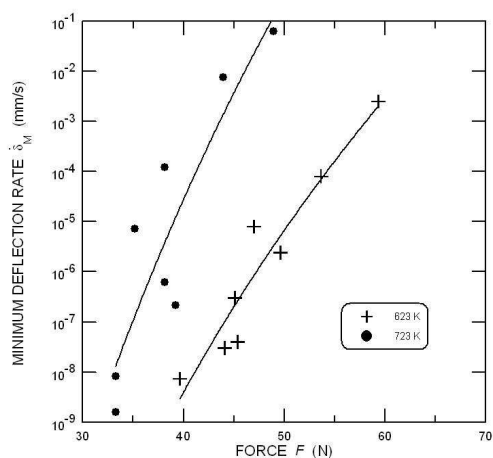
Fig. 12 Dependence of the minimum deflection rate on the applied force
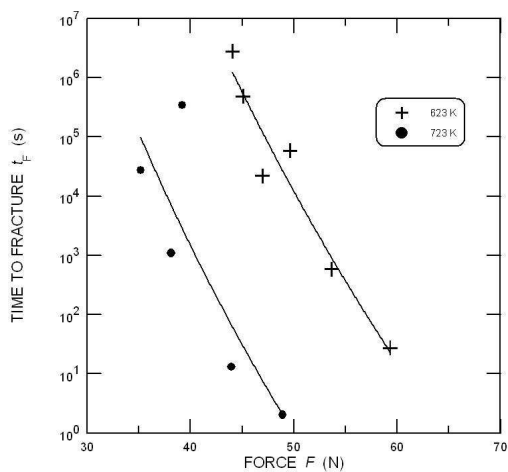
Fig. 13 Dependence of the time to fracture on the applied force

3.3 Mechanical properties of nanostructural system

The material after ECAP is on the border of nanostructural materials. Microstructure of the starting material is in **Fig. 14**. TEM micrograph, **Fig. 15** shows that the mean grain size was 100-200 nm, dislocations are present in nanograins, too, but mostly on the boundaries. In Fig. 15 these dislocations are weakly visible due to the tilting of the specimen. The nanostructure formation takes place most probably by a three-stage mechanism, described in [27]. This model has been experimentally verified only for several specific materials but in our case it seems to be probably usable. The model includes creation of cell structure, then formation of transitory cell nanostructure with large angle disorientation, and finally formation of nanostructural grains with size of approx. 100 nm. However, here one has to consider the retarding effect due to present dispersoid particles.

The composite was tested in two different states: a) as received by mechanical alloying with hot extrusion (HE) as the final operation and b) with ECAP superimposed on the hot extruded material, [28]. The ECAP does not improve the observed creep resistance. The reduction of force leading to the same deflection rate is not very significant. This points out that the ECAP process of the present composite, which produces substantial strengthening at lower temperatures, is not accompanied by pronounced weaking of creep resistance at elevated temperatures. The threshold force in the ECAP material is about 5 N weaker than in the HE material. The dependence of the minimum deflection rate on the applied force for two temperature levels is given in **Fig. 16**.
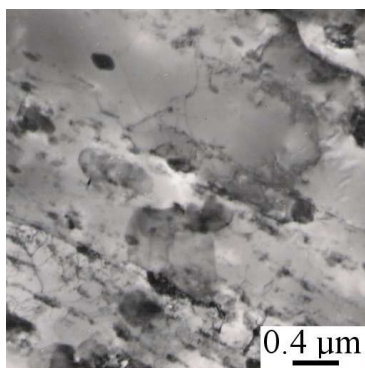
Fig. 14   Microstructure of the starting material
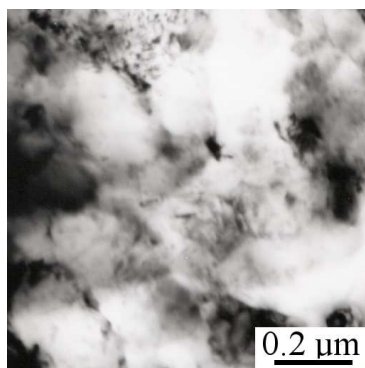
Fig. 15   Microstructure after ECAP
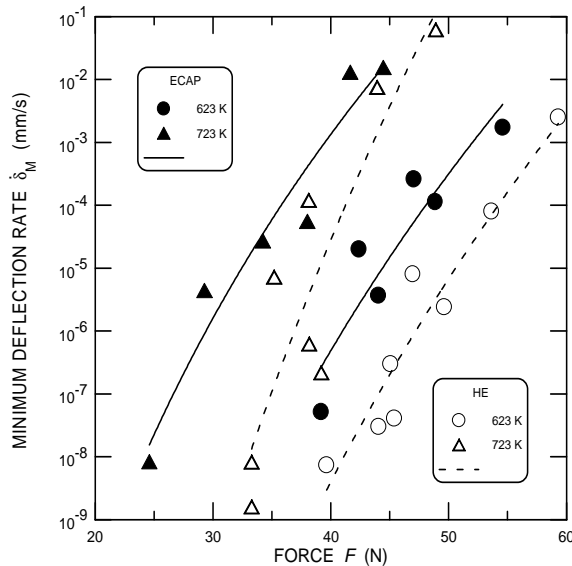
Fig. 16 Dependence of the minimum deflection rate on the applied force

The dependence can be described by the power-law relationship of the form:

$$\dot{\delta} = A_S \cdot F^{n_S} \,, \tag{2.}$$

where $\dot{\delta}$ is the minimum deflection rate, F is the acting force and A_S is a constant characterizing the temperature dependence. The values of the exponent n_S after hot extrusion, as reported previously [29], are 33.29 at 623 K and 41.56 at 723 K, respectively, and they are slightly lower after ECAP process: 29.0 at 623 and 23.4 at 723 K. Perhaps more significant is the fact that the deflection rate in ECAPed state is about two orders of magnitude faster than in the state not subjected to ECAP (64 times at 623 K; the exact value at 723 K is dependent on the applied force).

The dependence of the time to fracture, t_F on the applied force F is given in **Fig. 17**. The dependence can also be described by a power law of the type of (2), i. e.

$$t_F = A_F \cdot F^{n_F} \tag{3.}$$

with negative values of the power $n_F = -28.67$ at 623 K and -20.68 at 723 K. The absolute values of n_F are lower than values in hot extruded material reported previously (-36.59 at 623 K and -32.71 at 723 K, respectively). The times to fracture in ECAPed material are shorter than in the hot-extruded material, though the relative difference is smaller than in the previous case of deflection rate: Assuming the same value of power n_F in both materials, the time to facture is about 43 times shorter at 623 K and 14 times shorter at 723 K. The ratio at 723 K should be taken with caution since its force dependence has to be admitted.

The anisotropy of the creep properties and fracture using small punch tests for the Al-Al$_4$C$_3$ system produced by ECAP were analysed. Small punch creep tests under constant force were performed at the temperature of 623 K. It was shown that the fracture results, i.e. time to fracture

and deflection at fracture were different in specimen with different orientation with respect to the axis of ECAP deformation [30, 31]. A fracture surface analysis of the tested small punch specimens was conducted. Fractures have the transcrystalline ductile character. The fracture dimples are equiaxial as well as elongated in the dependence on strain direction. Fracture dimples are of two categories, the small ones sized from 0.1 to 0.5μm and large ones ranging from 3 to 6μm.
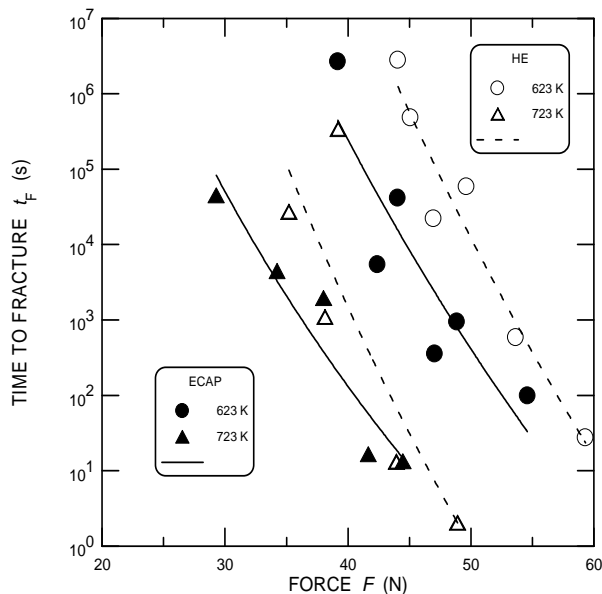
Fig. 17   Dependence of the time to fracture on the applied force

4   Conclusions

The results can be summarized as follows:

1. It was shown that the transformation efficiency of carbon to Al_4C_3 by heat treatment of aluminium with the porous furnace black *a)* and electrographite *b)* is higher, than that of the hard cracked graphite *c)*. Microstructure changes occurred in the fracture processes and welding the particles with incorporation of C phase and forming final granules.

2. The dispersed phase Al_4C_3 particle size was measured on thin foil structures, and it was constant and as small as 30 nm. The particle size was influenced neither by the carbon type nor by the heat treatment technology applied. Subgrain size measured in the range of 100 grains in thin foils depended on the carbon type, as well. It ranged from 0.3 to 0.7 μm.

3. The comparison of the tensile test results and changes in fracture for the Al-Al_4C_3 system at temperatures from 293 to 673 K and strain rates from $\dot{\varepsilon} = 2.5 \cdot 10^{-5}$ s^{-1} to $\dot{\varepsilon} = 1 \cdot 10^{-1}$ s^{-1} is summarized. The results are considered relevant to changes in micromechanism of deformation and fracture (transition from transcrystalline ductile fracture to intercrystalline fracture).

4. It follows from the model of superplastic deformation, that if the volume fraction of Al_4C_3 changes from lower to higher values, the grain rotation mechanism dominates instead of the grain boundary sliding.

5. Creep behaviour of the composite based on aluminium matrix, reinforced by 4 vol. % Al_4C_3

was studied at temperatures from 623 to 723 K by small punch (SP) testing with a constant force. The dependence of the minimum deflection rate on the applied force as well as the dependence of the time to fracture on the applied force was depicted.

6. The very fine-grained microstructure – nanostructure with the mean grain size of 100-200 nm was obtained a material $Al-Al_4C_3$ with 4 vol. % Al_4C_3 transformed by the ECAP technology by two passes.

7. The small punch tests of a mechanically alloyed Al composite with a superimposed ECAP procedure were performed in the constant force regime at the temperatures of 623 K and 723 K. The force dependencies of the minimum deflection rate and of the time to fracture are quantitatively comparable with the analogical dependencies of the hot extruded material. The ECAP does not improve the observed creep resistance. The anisotropy of the creep properties and fracture using small punch tests for the $Al-Al_4C_3$ system produced by ECAP were analyzed. A fracture surface analysis of the tested small punch specimens was conducted. Fractures have transcrystalline ductile character. The fracture dimples are equiaxial, elongated in the dependence on strain direction. Fracture dimples are of two categories, the small ones sized from 0.1 to 0.5 μm and large ones ranging from 3 to 6 μm.

References

[1] M. Besterci: *Dispersion strengthened aluminium prepared by mechanical alloying*, CISP, Cambridge, ISBN 189832655, 1999

[2] A. Orlová, K. Kuchařová, J. Čadek, M. Besterci, M. Šlesár: Kovove Materialy, Vol. 24, 1986, p. 505-529

[3] M. Besterci, G. Jangg, M. Šlesár, J. Zrník: Powder Metallurgy Progress, Vol. 1, 2001, p. 59-69

[4] J. S. Benjamin: Metallurgical and Materials Transactions A, Vol. 1, 1970, p. 2943-2951

[5] C. Suryanarayana: *Bibliography on Mechanical Alloying and Milling*, CISP, Cambridge, 1995

[6] G. Korb, G. Jangg, F. Kutner: Draht, Vol. 30, 1975, p. 318-324

[7] M. Besterci, M. Šlesár, G. Jangg, M. Miškovičová, J. Ďurišin: Kovove Materialy, Vol. 27, 1989, No. 1, p. 77-82

[8] R. Bidulsky, J. Bidulska, M. Actis Grande: High Temperature Materials and Processes, Vol. 28, 2009, No. 5, p. 337-342

[9] J. Bidulská et al.: Acta Metallurgica Slovaca, Vol. 16, 2010, No. 1, p. 4-11

[10] M. Besterci: Materials and Design, Vol. 27, 2006, p. 416-421, DOI: dx.doi.org/10.1016/j.matdes.2004.11.012

[11] I. Saxl, M. Besterci, K. Pelikán: Pokroky Práškové Metalurgie, Vol. 3, 1986, No. 4, p. 3-50

[12] I. Saxl, K. Pelikán, J. Rataj, M. Besterci: *Quantification and Modelling of Heterogenous Systems*, CISP, Cambridge, ISBN 1898326045, 1995

[13] M. Besterci, I. Kohútek, I. Saxl, K. Sülleiová: Journal of Materials Science, Vol. 34, 1999, p. 1055-1060

[14] A. Okabe, B. Boots, K. Sugihara: *Spatial Tessellation*, John Wiley & Sons, Chichester, 1992

[15] M. Besterci, J. Zrník, M. Šlesár: Kovove Materialy, Vol. 35, 1997, No. 5, p. 344-349

[16] M. Besterci, O. Velgosová, J. Ivan, L. Kováč: Kovove Materialy, Vol. 39, 2001, No. 5, p. 309-315

[17] R. S. Mishra, A. K. Mukherjee: Materials Science and Engineering A, Vol. 234-236, 1997, p. 1023-1025

[18] K. Higashi: Materials Science and Engineering A, Vol. 166, 1993, p. 109-118

[19] M. Besterci, O. Velgosová, L. Kováč, J. Ivan: Materials Science Forum, Vol. 416-418, 2003, p. 207-212

[20] O. Velgosová, M. Besterci, L. Kováč, P. Kulu, S.J. Huang: Kovove Materialy, Vol. 49, 2011, No. 5, p. 361-367, DOI: 10.4149/km20115361

[21] M. Besterci, J. Čadek: High Temperature Materials and Processes, Vol. 23, 2004, No. 1, p. 51-57

[22] F. Dobeš, K. Milička: Metal Science, Vol. 10, 1976, p. 382-382

[23] A. Orlová, K. Kuchařová, J. Čadek: Kovove materialy, Vol. 27, 1989, p. 3-27

[24] J. Čadek: Materials Science and Engineering A, Vol. 117, L5, 1989

[25] G. E. Lucas: Metallurgical Transactions A, Vol. 21, 1990, No. 4, p. 1105-1119, DOI: 10.1007/BF02656531

[26] J. M. Baik, J. Kameda, O. Buck: Scripta Metallurgica, Vol. 17, 1983, p. 1443-1447

[27] R. Z. Valiev, I. V. Alexandrov: Nanostructure materials obtained by SPD, Logos, Moskva, 2000, (in Russian)

[28] F. Dobeš, K. Milička, M. Besterci, T. Kvačkaj: Journal of Materials Science, Vol. 45, 2010, p. 5171-5176, DOI:10.1007/s10853-010-4554-9

[29] F. Dobeš, K. Milička, M. Besterci: High Temperature Materials and Processes, Vol. 26, 2007, No. 3, p. 193-199, DOI: 10.1515/HTMP.2007.26.3.193

[30] M. Besterci, F. Dobeš, B. Ballóková, K. Sülleiová, T. Kvačkaj: High Temperature Materials and Processes, Vol. 30, 2011, p. 205-210, DOI: 10.1515/HTMP.2011.030

[31] M. Besterci, K. Sülleiová, T. Kvačkaj: Kovove Materialy, Vol. 46, 2007, No. 5, p. 309-311